Phase Locked Loop with Multifrequency Phase Unwrapping Structure

Sébastien Roche[1], Stéphanie Bidon[1], Michel Monnerat[2], Lionel Ries[3] and Paul Thevenon [3]
[1] TéSA-ISAE, Toulouse, France
mail: sebastien.roche@isae.fr
[2]Thales Alenia Space, France
[3]CNES, Toulouse, France

***Abstract*—For precise positioning techniques, performance of phase lock loop (PLL) is of utmost importance since the estimated receiver's position is intimately linked to phase measurement. Unfortunately, conventional PLLs suffer from a lack of noise robustness that is mostly due to cycle slips. Cycle slips are phase measurement biases that occur during the phase tracking and damage the quality of phase estimation. The purpose of this paper is to propose a new PLL design embedding a multifrequency phase unwrapping technique. Indeed, with the modernization of GPS and the arrival of the future European positioning system Galileo, users will have access to numerous civilian multicarrier signals. We exploit this diversity within a phase unwrapping structure that allows the incoming phase dynamics to be predicted and subsequently the dynamics estimated by the discriminator to be reduced. Compared with a conventional PLL, this new structure offers a better cycle slip robustness and reduces the probability of loss of lock.**

BIOGRAPHIES

Sébastien Roche graduated as an aeronautical engineer from the ISAE-ENSICA in 2010. He is now a Ph.D. student at the University of Toulouse. Currently he carries out research on robust PLL structure in collaboration with the CNES (Centre National d'Etudes Spatiales) and Thales Alenia Space, in Toulouse, France.

Stéphanie Bidon received the Ph.D. degree from INP, Toulouse, in 2008. She is now with the Department of Electronics, Optronics and Signal of ISAE (Institut Supérieur de l'Aéronautique et de l'Espace, Toulouse) as an assistant professor. Her research interests include digital signal processing particulary with application to airborne radar.

Michel Monnerat, Location Infrastructure and Security Manager at Thales Alenia Space. After working on many radar programs within Alcatel Space, and after being in charge of the onboard processing of the ARGOS/SARSAT payloads, he has been involved in the Galileo program since 1998, particularly for the signal design and performance aspects. He is now in charge of research and development for new location technologies and infrastructure, developing high quality of service (QoS) positioning solutions.

Lionel Ries is head of the Signal and RadioNavigation department of the CNES Radiofrequency sub-directorate since August 2009. He was a navigation engineer in the Transmission Techniques and Signal Processing department, at CNES since June 2000. He is one of the CBOC inventors. He graduated from the Ecole Polytechnique de Bruxelles, at Brussels Free University (Belgium) and received a M.S. degree from ISAE in Toulouse (France).

Paul Thevenon Paul Thevenon is GNSS engineer in the GNSS signal processing team of CNES (Centre National d'Etudes Spatiales), the French space research center. He graduated as electronic engineer from Ecole Centrale de Lille in 2004 and obtained in 2007 a research master at ISAE (Institut Supérieur de l'Aéronautique et de l'Espace) in space telecommunications. In 2010, he obtained a PhD degree in the signal processing laboratory of ENAC (Ecole Nationale de l'Aviation Civile) in Toulouse, France by studying the feasibility of self-positioning a receiver using mobile TV signals. His current activity is GNSS signal measurement and processing, with an emphasis on urban environment.

I. INTRODUCTION

Precise Point Positioning (PPP) techniques are able to provide accurate user positioning with a single receiver. To obtain centimeter-level accuracy, PPP algorithms need accurate orbital and clock data of the satellites in view as well as carrier phase observations collected by the user's receiver [1]. Although mass market applications "hunger" for precise positioning, PPP methods are not yet implemented for such applications. Indeed carrier phase estimation, ensured for instance by phase lock loops (PLL), suffers from a lack of robustness in case of low carrier-to-noise-density-ratio (CN0) environments such as urban canyons.

The weak noise robustness of phase tracking is partially due to the presence of cycle slips that can cause the loss of lock. Cycle slip phenomenon is a distinctive characteristic of PLLs which directly results from the periodic nature of phase discriminators used in tracking loops [2]. These phase bias are caused by either a high dynamic stress and/or a high noise level. Simple methods have been proposed to correct cycle slips caused by a high dynamic stress within the PLL. They rely mostly on a fixed thresholding procedure (i.e., use of sawtooth function at the discriminator output) [3], [4]. However, PLLs based on such non-linear techniques can wrongly induce cycle slips in case of noisy environments.

Recently we have proposed a new PLL design that embeds a phase unwrapping structure based on a polynomial prediction algorithm for cycle slips anticipation [5]. More precisely, this structure (which tracks the phase of a single-carrier signal) aims at predicting the discriminator output by analyzing the former loop filter outputs thanks to a polynomial model. The polynomial coefficients are estimated via the weighted recursive least squares (WRLS). Once the next discriminator output is estimated, the prediction is pre-compensated so that the phase dynamics to be tracked is reduced. Compared with conventional PLL structures, our PLL structure allowed the cycle slip rate and the probability of loss of lock to be decreased.

In this paper, we propose to extend our former unwrapping structure [5] to multifrequency signals so as to enhance the tracking performance of their associated PLLs. In the foreseeable future, a large diversity of multifrequency signals will be accessible to civilian receivers for many navigation constellations (e.g., L1, L1C, L2C and L5 GPS signals, E1, E5a, E5b and E6 Galileo signals). Frequency diversity is known to offer many advantages, e.g., improved integrity and robustness towards jammers, ionosphere estimation capabilities and multipath mitigation. It offers also the possibility to observe the relative radial velocity of the user as many times as there are transmitted frequencies [10]. More specifically, carrier phases received from the same satellite are supposed, up to a multiplicative constant and in absence of strong ionospheric scintillation, to be equal. By relying on this property and taking advantage of the subsequent proportionality relationship that takes place between the observed Doppler frequencies (defined as the derivative of the carrier phases), two new PLL structures with a multifrequency phase unwrapping technique are presented in this paper.

The remaining of the paper is organized as follows. Section 2 describes the model of the incoming multifrequency signal. Section 3 details the two multifrequency PLL structures proposed herein. Section 4 is a comparative study which highlights the efficiency of the two proposed multicarrier structures in terms of noise robustness. Finally, Section 5 concludes the paper.

II. Received signal model

The incoming signal is a multifrequency signal related to P carrier frequencies emitted by the same satellite. The signal component associated with each carrier is assumed to be a complex exponential signal and received on an independent RF channel. Code delay and data navigation synchronization are supposed to be perfectly established so that the signal model does not include neither Gold codes nor navigation data bits. The incoming signal related to the pth frequency can therefore be expressed as

$$s_p[k] = \sqrt{C_p} e^{2i\pi\theta_p[k]} + n_p[k] \tag{1}$$

with C_p the received signal power, $\theta_p[k]$ the (normalized) carrier phase to be tracked and $n_p[k]$ the white Gaussian thermal noise defined as

$$n_p \sim \mathcal{CN}\left(0, \sigma_p^2\right). \tag{2}$$

The thermal noise power σ_p^2 is given by

$$\sigma_p^2 = \frac{C_p}{CN0_p} F_s, \tag{3}$$

with $CN0_p$ the carrier-to-noise-density-ratio of the pth frequency and F_s the incoming signal sample rate. The received phase θ_p is supposed to be related to two additive phenomena, i.e., the Doppler effect and ionospheric perturbations, so that it can be expressed as follows

$$\theta_p = \theta_p^{Doppler} + \Delta\theta_p^{iono} \tag{4}$$

where each component can be easily identified by its superscript. Accordingly, the phase rate associated with the model (4) is given by

$$\begin{aligned} \dot{\theta}_p &= \frac{d\theta_p}{dt}, \\ &= \dot{\theta}_p^{Doppler} + \Delta\dot{\theta}_p^{iono} \end{aligned}$$

where $\dot{\theta}_p^{Doppler}$ is the conventional Doppler frequency [10], i.e.,

$$\dot{\theta}_p^{Doppler} = -f_p \frac{\boldsymbol{v}^T \boldsymbol{a}}{c} \tag{5}$$

with f_p the carrier frequency of the pth frequency, $\boldsymbol{v}$ the satellite-to-user relative velocity vector, $\boldsymbol{a}$ the unit vector pointing along the line of sight from the user to the satellite, and c the speed of light. The term $\Delta\dot{\theta}_p^{iono}$ is related to the change rate of the ionospheric electrical content. By assuming that the received signal is tracked under non-critical ionospheric condition, $\Delta\dot{\theta}_p^{iono}$ is generally slow enough to be neglected [6]. Thus, the phase rate is simply given by

$$\dot{\theta}_p = -f_p \frac{\boldsymbol{v}^T \boldsymbol{a}}{c}. \tag{6}$$

Recalling that the P frequencies are assumed to be emitted by the same satellite, the term $\boldsymbol{v}^T\boldsymbol{a}/c$ has the same value. This leads to a proportionality relationship between θ_p and $\theta_{p'}$ as [7]

$$\dot{\theta}_p = \frac{f_p}{f_{p'}} \dot{\theta}_{p'} \tag{7}$$

where f_p and $f_{p'}$ are the pth and p'th frequencies respectively.

III. PLLs with multifrequency phase unwrapping structure

In this section, we propose two new PLL structures that incorporate a phase unwrapping technique using frequency diversity. These PLLs are extended versions of a former design proposed in case of single-frequency signal [5]. We recall first the single-frequency approach before describing its extended versions to multi-frequency scenario.

A. The single-carrier structure

The multifrequency structures proposed in this paper are inspired from the phase unwrapping structure illustrated in figure 1. This single-frequency structure is based on a conventional PLL. An external system is added to the conventional structure to reduce the dynamics estimated by the discriminator. This system aims at predicting the forward phase discriminator output by analyzing the loop filter outputs. By reducing the dynamics to be tracked, cycle slip rate is reduced and makes the PLL of figure 1 more robust than conventional PLL.

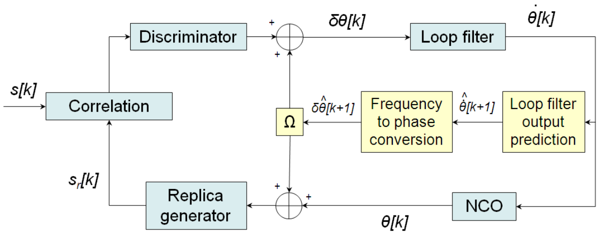

Figure 1: PLL structure with single-frequency phase unwrapping [5]

To analyze the frequency dynamics estimated by the loop filter (i.e., the loop filter outputs), an analysis model had been chosen as

$$\dot{\theta}[k] = \sum_{m=0}^{M} b_m k^m + \nu[k], \tag{8}$$

with $\dot{\theta}$ the loop filter output, ν the noise component, M the degree of the polynomial analysis model (generally chosen as $M = 1$) and $\{b_0 \dots b_M\}$ the polynomial coefficients. This polynomial model enforces smoothness and allows us, by estimating the parameters $\{b_0 \dots b_M\}$, to predict the next frequency estimate $\hat{\dot{\theta}}[k+1]$. Once the forward frequency output is estimated, a conversion step estimates the next discriminator output by using the polynomial parameters $\{b_0 \dots b_M\}$. This calculation step uses the closed-loop transfer function of the conventional PLL to express the discriminator output as a function of the incoming dynamics (i.e., the polynomial parameters) [5]. Finally, a gain Ω is added before precompensating the discriminator prediction to reduce prediction error effect. Obviously, this gain will be chosen such as $\Omega < 1$.

The algorithm that recursively estimates the polynomial coefficients is the WRLS algorithm described in [5].

B. Multicarrier structures

To design a multicarrier PLL structure based on the prediction/pre-compensation system as described in [5] and illustrated in figure 1, frequency observations (i.e., outputs of the loop filters) have to be analyzed by the analysis model (8). To do so, we propose two different approaches denoted respectively as centralized and decentralized estimation which are detailed hereafter. In both approaches, PLLs associated with each transmitted frequency are run in parallel.

1) First multicarrier PLL structure: centralized estimation

The multicarrier PLL structure associated with the centralized approach is illustrated in figure 2.

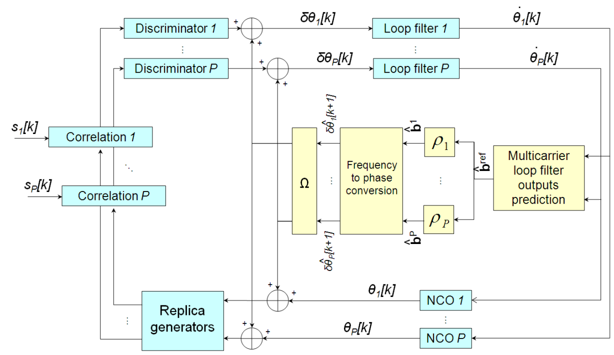

Figure 2: Multifrequency PLL structure in case of a centralized approach

In the centralized approach, a unique estimation step is performed. The relation of proportionality (7) is directly considered so that only one set of polynomial coefficients is actually estimated. To do so, a WRLS algorithm suited for multi-frequency signals has been developed. More precisely, let us assume that we have access to the P observation vectors $\boldsymbol{y}_p$ $(p = 1, \dots, P)$ associated with the N first loop filter outputs of the P PLLs tracking the multicarrier signal

$$\begin{aligned} \boldsymbol{y}_{1,N} &= \left[\dot{\theta}_1[0] \dots \dot{\theta}_1[N-1]\right]^T \\ &\vdots \\ \boldsymbol{y}_{P,N} &= \left[\dot{\theta}_P[0] \dots \dot{\theta}_P[N-1]\right]^T. \end{aligned} \tag{9}$$

Since we are searching to estimate a unique set of coefficients $\{b_1, \dots, b_M\}$, we use the relation of proportionality (7) as proposed hereafter. We choose a reference frequency f_{ref} among the P frequencies and rewrites all the Doppler frequencies as

$$\dot{\theta}_p = \rho_p \dot{\theta}_{\text{ref}} \tag{10}$$

where

$$\rho_p = \frac{f_p}{f_{\text{ref}}}. \tag{11}$$

Then using relation (10) while assuming a polynomial model for the time-evolution of the pth phase yields

$$\begin{aligned} \dot{\theta}_p[k] &= \sum_{m=0}^{M} b_m^p k^m + \nu_p[k], && (12) \\ &= \rho_p \sum_{m=0}^{M} b_m^{\text{ref}} k^m + \nu_p[k], && (13) \end{aligned}$$

The following vector notation is finally obtained

$$\boldsymbol{H}_N \boldsymbol{b}_N^{\text{ref}} + \boldsymbol{\nu}_N = \boldsymbol{y}_N \tag{14}$$

with $\boldsymbol{\nu}_N$ the noise vector

$$\begin{aligned}\boldsymbol{y}_N &= [\boldsymbol{y}_{1,N}^T, \cdots, \boldsymbol{y}_{P,N}^T]^T \\ \boldsymbol{b}_N^{\text{ref}} &= [b_0^{\text{ref}}(N), \cdots, b_M^{\text{ref}}(N)]^T \\ \boldsymbol{H}_N &= \boldsymbol{\rho} \otimes \boldsymbol{G}_N\end{aligned}$$

where

$$\boldsymbol{\rho} = [\rho_1, \cdots, \rho_P]^T, \tag{15}$$

$$\boldsymbol{G}_N = \begin{bmatrix} 1 & 0 & 0^2 & \cdots & 0^M \\ \vdots & \vdots & \vdots & \vdots & \\ 1 & (N-2) & (N-2)^2 & \cdots & (N-2)^M \\ 1 & (N-1) & (N-1)^2 & \cdots & (N-1)^M \end{bmatrix}.$$

The weighted least squares estimation problem for the reference polynomial coefficients $\boldsymbol{b}^{\text{ref}}$ is

$$\hat{\boldsymbol{b}}_N^{\text{ref}} = \arg \min_{\boldsymbol{b}} \left[(\boldsymbol{H}_N \boldsymbol{b} - \boldsymbol{y}_N) \boldsymbol{R}_N^{-1} (\boldsymbol{H}_N \boldsymbol{b} - \boldsymbol{y}_N)^T \right]$$

with $\boldsymbol{R}_N$ the $NP \times NP$ weighted matrix defined as

$$\boldsymbol{R}_N^{-1} = \begin{pmatrix} \boldsymbol{R}_{1,N}^{-1} & & \\ & \ddots & \\ & & \boldsymbol{R}_{P,N}^{-1} \end{pmatrix}, \tag{16}$$

where $\boldsymbol{R}_{p,N}^{-1}$ is the $N \times N$ weight matrix associated with the frequency f_p. In our study, we choose

$$\boldsymbol{R}_{p,N}^{-1} = \begin{pmatrix} 1 & & \\ & \ddots & \\ & & \lambda^{N-1} \end{pmatrix}, \tag{17}$$

where λ is the weight factor chosen as $\lambda < 1$ to give more importance to the latest observations. Estimate of the reference polynomial coefficients $\boldsymbol{b}^{\text{ref}}$ is given by [12]

$$\hat{\boldsymbol{b}}_N^{\text{ref}} = \left(\boldsymbol{H}_N^T \boldsymbol{R}_N^{-1} \boldsymbol{H}_N \right)^{-1} \boldsymbol{R}_N^{-1} \boldsymbol{H}_N^T \boldsymbol{y}_N. \tag{18}$$

During the phase tracking, the reference coefficients vector can be recursively estimated by updating the estimate $\hat{\boldsymbol{b}}_N^{\text{ref}}$ thanks to the new observations $\{y_{1,N+1}, \dots, y_{P,N+1}\}$. Details of the WRLS algorithm that has been developed to estimate the coefficient vector in case of a multicarrier approach are given in Appendix. Once the estimation of the coefficient vector $\hat{\boldsymbol{b}}^{\text{ref}}$ is performed, the coefficient vectors associated with the P frequencies are built as follows for each frequency f_p

$$\hat{\boldsymbol{b}}^p = \rho_p \hat{\boldsymbol{b}}^{\text{ref}}.$$

The coefficient vectors can thus be used to pre-compensate the phase dynamics estimated by the discriminator of the PLLs they are associated with.

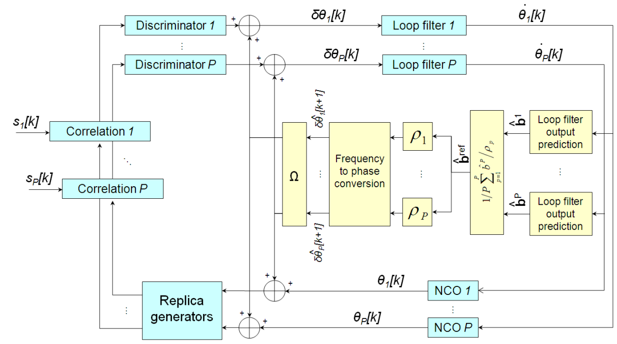

Figure 3: Multifrequency PLL structure in case of a decentralized approach

2) Second multicarrier PLL structure: decentralized estimation

The multicarrier PLL structure associated with the decentralized approach is illustrated in figure 3.

As for the first solution previously described, the decentralized approach uses the proportionality relationship (7) that takes place between the Doppler frequencies. However, here, polynomial coefficients are firstly estimated independently for each carrier. This set of coefficients is then re-estimated while enforcing a known relation of proportionality between them. More precisely, let us suppose that we have P PLLs (associated with the P transmitted signals) that are run in parallel. The model (8) can be used to analyze, as in the single-frequency approach, the loop filter outputs of each PLL. By doing so, we estimate the P coefficient vectors

$$\begin{aligned}\hat{\boldsymbol{b}}^1 &= [\hat{b}_0^1, \cdots, \hat{b}_M^1]^T \\ &\vdots \\ \hat{\boldsymbol{b}}^P &= [\hat{b}_0^P, \cdots, \hat{b}_M^P]^T.\end{aligned} \tag{19}$$

Due to the proportionality relationship between Doppler frequencies (7), the estimated set of coefficients are also supposed to be proportional. By choosing the coefficient vector $\boldsymbol{b}^{\text{ref}}$ as the reference vector, one can write

$$\begin{aligned}\boldsymbol{b}^1 &= \rho_1 \boldsymbol{b}^{\text{ref}}, \\ &\vdots \\ \boldsymbol{b}^P &= \rho_P \boldsymbol{b}^{\text{ref}},\end{aligned} \tag{20}$$

where

$$\boldsymbol{b}^{\text{ref}} = [b_0^{\text{ref}}, \cdots, b_M^{\text{ref}}]^T,$$

and ρ_p is the carrier frequency ratio defined in (11). To estimate $\boldsymbol{b}^{\text{ref}}$, we propose to simply combined the P estimated vectors $\boldsymbol{b}^p$ as follows

$$\hat{\boldsymbol{b}}^{\text{ref}} = \frac{1}{P} \sum_{p=1}^{P} \frac{\hat{\boldsymbol{b}}^p}{\rho_p}. \tag{21}$$

Once the estimation of the coefficient vector $\hat{\boldsymbol{b}}^{\text{ref}}$ is performed, the coefficient vectors associated with the different carrier frequencies are given by

$$\hat{\boldsymbol{b}}^p = \rho_p \hat{\boldsymbol{b}}^{\text{ref}}.$$

The coefficient vectors can thus be used to pre-compensate the phase dynamics estimated by the discriminator of the PLLs they are associated with.

IV. Numerical simulations

In this section, we study the performance of the two multicarrier PLL structures presented in Section 3. To highlight their robustness, we compare them to the single-carrier unwrapping structure they are inspired from (this structure is illustrated in figure 1). In the following, a Doppler carrier phase dynamics will be fixed and tracked by all the PLLs for different $CN0$ values.

A. Description of the simulations

For the simulations that follow, the incoming multicarrier signal is generated as described in (1). Here, we only consider the case of a bifrequency signal composed of the L1 (1575.42 MHz) and L2 (1227.6 MHz) frequencies. The Doppler phase dynamics associated with the pth carrier is generated as

$$\theta_p[k] = \dot{\theta}_p(0)kT_s + \frac{1}{2}\ddot{\theta}_p(0)k^2T_s^2, \tag{22}$$

with

$$\begin{aligned} \dot{\theta}_{L_1}(0) &= 3Hz, \\ \ddot{\theta}_{L_1}(0) &= 1Hz/s, \\ \left[\dot{\theta}_{L_2}(0), \ddot{\theta}_{L_2}(0)\right] &= \frac{f_{L_2}}{f_{L_1}}\left[\dot{\theta}_{L_1}(0), \ddot{\theta}_{L_1}(0)\right]. \end{aligned}$$

For the analysis model of the loop filter outputs, the polynomial degree M is fixed to 1 so that the frequency outputs can be approximated by a linear relation viz

$$\dot{\theta}_p[k] = b_0^p + b_1^p k. \tag{23}$$

The discriminator used for the three considered PLLs is the ATAN discriminator [10]. The loop bandwidth is fixed at $B_L = 5Hz$ (high enough to estimate the Doppler phase dynamics) and the correlation time at $T_{\text{corr}} = 20$ ms. The WRLS weight factor λ and the corrective gain Ω are fixed to $\lambda = 0.8$ and $\Omega = 0.6$.

To compare the noise robustness of the proposed structures, two performance metrics are considered: the loss of lock probability and the cycle slip rate (based on the tracking time before losing the lock).

B. Results

Figure 4 shows the performance (obtained thanks to Monte-Carlo simulations) of the studied PLLs for 20 seconds of track when the two frequencies (L1 and L2) are received under identical $CN0$ conditions (i.e., $CN0_{L1} = CN0_{L2}$). We can see that, compared to the single-frequency structure, the two proposed multifrequency structures offer an improved noise robustness. More precisely, for reasonable CN0 values, loss of lock probabilities on L1 and L2 are decreased as well as the cycle slip rates. One can notice that the performance improvement depends on the carrier frequency. Indeed, the L1 carrier benefits more from the multicarrier tracking

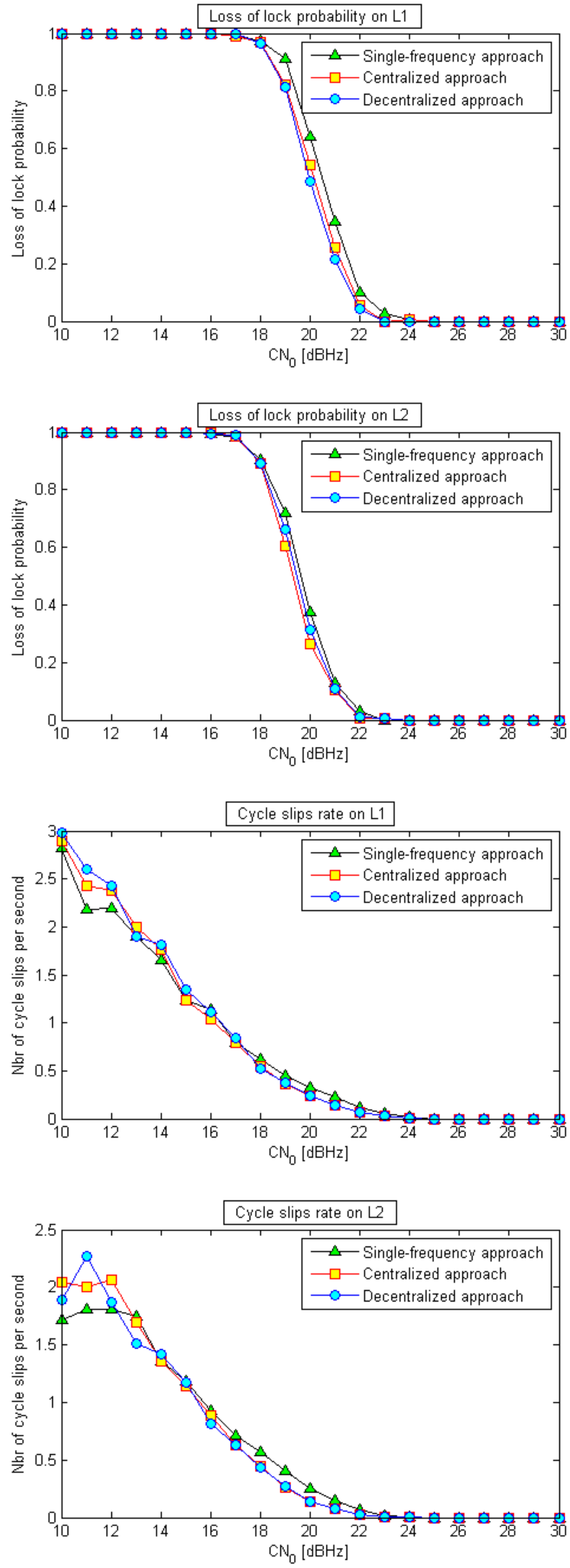

Figure 4: Tracking performance of PLLs with different phase unwrapping structures. Single- vs multi-frequency approaches (L1 and L2 have the same power)

Table 1: L1 and L2 received minimum RF signal strength

	L1C	L2C
Received power [dBW]	-158.5	-161, -163

approach in terms of loss of lock probability. This result can be easily explained by the fact that the Doppler dynamics on L1 is higher than the L2 dynamics. An improved dynamics estimation and reduction is thus more profitable for the highest frequency L1. On the other hand, figure 4 shows that the cycle slip correction is better on L2. This observation, which contrasts with the performance improvement on loss of lock probability, can be explained by considering the noise prediction on frequency dynamics. Indeed, whatever the multicarrier tracking approach we choose, the frequency dynamics is estimated via a reference polynomial coefficient vector $\hat{\boldsymbol{b}}^{\text{ref}}$. To compute the coefficient vector associated with the pth carrier frequency, we use the different frequency ratio ρ_p. Knowing that $\rho_{L1} > \rho_{L2}$, the prediction error (injected in the tracking via the pre-compensation system) is thus lower for the L2 carrier frequency. In our simulation scenario, cycle slips mainly occur due to noise (loop bandwidth is high enough to track the phase dynamics). Consequently, if the prediction error is higher on L1, it makes sense that the cycle slip rate is lower on L2.

In practice, the two carrier frequencies L1 and L2 may not be received under the same $CN0$ conditions. The L1 and L2 received minimum RF signal strengths are given in table 1 [14]. This difference of power can be profitable for the weakest carrier frequency in case of a multicarrier tracking approach. Indeed, one can expect that the strongest frequency may help the weakest one to improve its tracking performance thanks to the common dynamics prediction system (same idea has lead to the development of vector-tracking approaches [6]). To check this assumption, let us track the carrier phase from the L1 and L2 frequencies in a case where $CN0_{L1}$ differs from $CN0_{L2}$. In accordance with table 1, we choose $CN0_{L1} = CN0_{L2} + 5$ dBHz. Tracking performance for this new scenario is illustrated in figure 5. It shows that, for the multifrequency approaches, the weakest frequency has its performance significantly improved while the strongest one sees its performance decreased both in terms of cycle slipping rate and loss of lock probability. This result confirms that the proposed multicarrier structures are profitable for the carrier with the weakest power. However, it is worth noticing that the strongest frequency is polluted by the weakest channel. It could be thus advantageous to consider a mixed approach where the strongest channel would assist the weakest one but not reciprocally (to avoid any contamination). Decision to track a channel with a multi or a single-frequency approach could be determined by estimating the CN0 of the different frequencies thanks to a loop signal-to-noise-ratio estimator [13].

Concerning the relative tracking performance of the two proposed multicarrier structures, it can be seen in figures 4 and 5 that there is no significant difference between the two tracking approaches. Knowing that, the decentralized approach seems to be the best solution for multifrequency

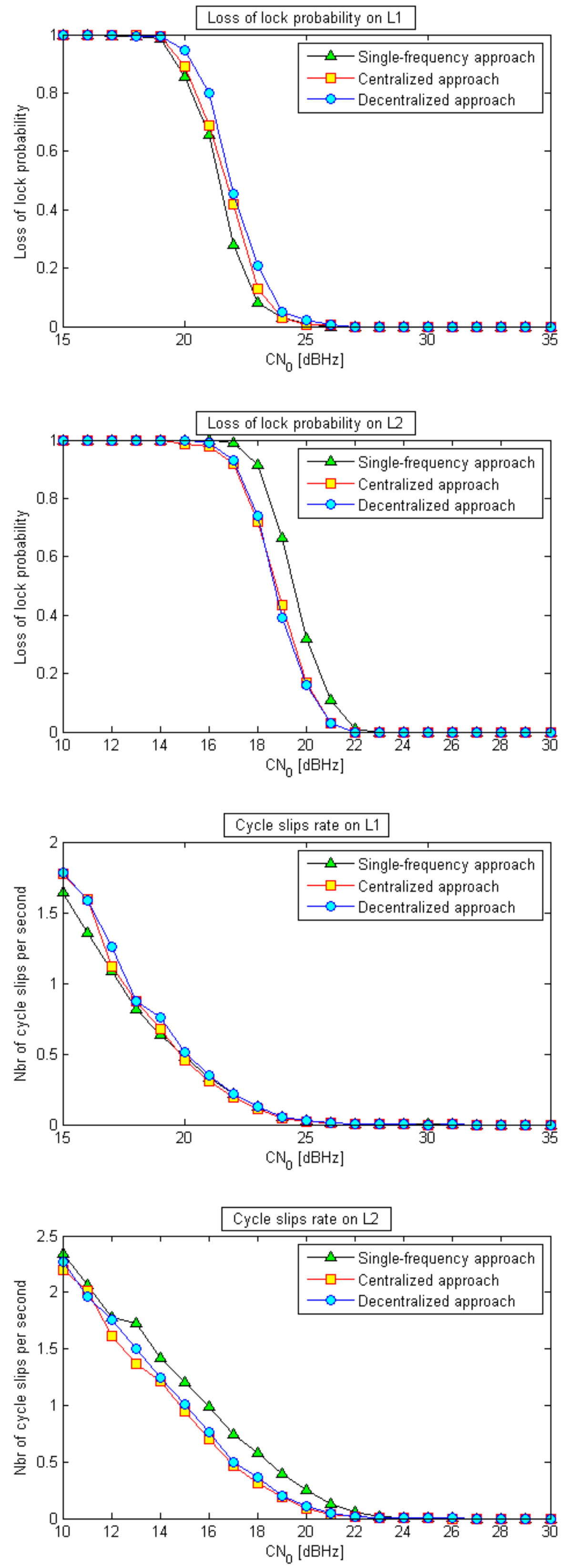

Figure 5: Tracking performance of PLLs with different phase unwrapping structures. Single- vs multi-frequency approaches (L1 has a higher power than L2)

signal tracking because of the lower complexity of its data combination system.

V. Conclusion

Phase tracking is a delicate but essential task to obtain accurate GNSS positioning. In particular cycle slips in phase-locked loops have a very detrimental effect on the performance of phase measurement. To avoid cycle slips, we have proposed in this paper two new PLL structures that incorporate a multi-frequency phase unwrapping system. In both structures, the phase dynamics to be tracked is decreased via a system of prediction that exploits frequency diversity either in a centralized or decentralized approach. Numerical simulations showed that the two proposed structures offer improved noise robustness by reducing the loss of lock probability as well as the cycle slip rate. Interestingly, it was shown that when a multi-frequency signal is received with different power (with respect to the frequency), the channel corresponding to the strongest frequency is able to assist the weakest one. However, reciprocally, the weakest channel contaminates the strongest one. Future works will therefore focus on defining new multi-frequency tracking strategy capable of weighting the assistance between channels according to integrity indicator.

Acknowledgment

This work was supported by the French space research agency CNES (Centre National d'Etudes Spatiales) and Thales Alenia Space, France.

Appendix

This Appendix gives the expression of the WRLS algorithm which allows us to recursively estimate the coefficient vector $\boldsymbol{b}^{\text{ref}}$. Matrices and vectors notations are the same as previously introduced in section III.

Let us assume that, at the instant N, we have access to the $N \times P$ first loop filter outputs associated with the N first loop filter outputs of the P PLLs tracking the multicarrier signal

$$\begin{aligned}\boldsymbol{y}_{1,N} &= \left[\dot{\theta}_1[0] \dots \dot{\theta}_1[N-1]\right]^T \\ &\vdots \\ \boldsymbol{y}_{P,N} &= \left[\dot{\theta}_P[0] \dots \dot{\theta}_P[N-1]\right]^T.\end{aligned}$$

The estimate of the $(M+1) \times 1$ coefficient vector $\boldsymbol{b}_N^{\text{ref}}$ is

$$\hat{\boldsymbol{b}}_N^{\text{ref}} = \left(\boldsymbol{H}_N^T \boldsymbol{R}_N^{-1} \boldsymbol{H}_N\right)^{-1} \boldsymbol{R}_N^{-1} \boldsymbol{H}_N^T \boldsymbol{y}_N,$$

where

$$\boldsymbol{y}_N = [\boldsymbol{y}_{1,N}^T, \cdots, \boldsymbol{y}_{P,N}^T]^T,$$

$$\boldsymbol{R}_N^{-1} = \begin{pmatrix} \boldsymbol{R}_{1,N}^{-1} & & \\ & \ddots & \\ & & \boldsymbol{R}_{P,N}^{-1} \end{pmatrix},$$

$$\boldsymbol{H}_N = \boldsymbol{\rho} \otimes \boldsymbol{G}_N$$

whose sizes are respectively $NP \times 1$, $NP \times NP$ and $NP \times (M+1)$.

At the instant $N+1$, if we have access to the $(N+1) \times P$ observations

$$\begin{aligned}\boldsymbol{y}_{1,N+1} &= \left[\boldsymbol{y}_{1,N}^T, y_{1,N+1}\right]^T \\ &\vdots \\ \boldsymbol{y}_{P,N+1} &= \left[\boldsymbol{y}_{P,N}^T, y_{P,N+1}\right]^T\end{aligned}$$

the new estimate of the polynomial coefficients $\boldsymbol{b}_{N+1}^{\text{ref}}$ at the instant $N+1$ is

$$\hat{\boldsymbol{b}}_{N+1}^{\text{ref}} = \left(\boldsymbol{H}_{N+1}^T \boldsymbol{R}_{N+1}^{-1} \boldsymbol{H}_{N+1}\right)^{-1} \boldsymbol{R}_{N+1}^{-1} \boldsymbol{H}_{N+1}^T \boldsymbol{y}_{N+1},$$

where

$$\begin{aligned}\boldsymbol{y}_{N+1} &= [\boldsymbol{y}_{1,N+1}^T, \cdots, \boldsymbol{y}_{P,N+1}^T]^T, \\ &= [\boldsymbol{y}_{1,N}^T, y_{1,N+1}, \cdots, \boldsymbol{y}_{P,N}^T, y_{P,N+1}]^T,\end{aligned}$$

$$\boldsymbol{R}_{N+1}^{-1} = \begin{pmatrix} \boldsymbol{R}_{1,N}^{-1} & & & & \\ & r_{1,N+1}^{-1} & & & \\ & & \ddots & & \\ & & & \boldsymbol{R}_{P,N}^{-1} & \\ & & & & r_{1,N+1}^{-1} \end{pmatrix},$$

$$\begin{aligned}\boldsymbol{H}_{N+1} &= \boldsymbol{\rho} \otimes \boldsymbol{G}_{n+1}, \\ \boldsymbol{G}_{N+1} &= \begin{pmatrix} \boldsymbol{G}_N \\ \boldsymbol{g}_{N+1} \end{pmatrix},\end{aligned}$$

with

$$\boldsymbol{g}_{N+1} = [1, \dots, N^M].$$

To recursively estimate the vector $\boldsymbol{b}^{\text{ref}}$ during the tracking, the estimated vector $\hat{\boldsymbol{b}}_{N+1}^{\text{ref}}$ has to be calculated as a function of $\hat{\boldsymbol{b}}_N^{\text{ref}}$. To do so, we use the WRLS algorithm that, in our case, is given by two recursive steps (and a initialization step) detailed hereafter.

0-Initialization ($N = N_{\text{init}} > M$)

$$\begin{aligned}\hat{\boldsymbol{b}}_{N_{\text{init}}}^{\text{ref}} &= (\boldsymbol{H}_{N_{\text{init}}}^T \boldsymbol{R}_{N_{\text{init}}}^{-1} \boldsymbol{H}_{N_{\text{init}}})^{-1} \boldsymbol{H}_{N_{\text{init}}}^T \boldsymbol{R}_{N_{\text{init}}}^{-1} \boldsymbol{y}_{N_{\text{init}}} \\ \boldsymbol{P}_{N_{\text{init}}} &= (\boldsymbol{H}_{N_{\text{init}}}^T \boldsymbol{R}_{N_{\text{init}}}^{-1} \boldsymbol{H}_{N_{\text{init}}})^{-1}\end{aligned}$$

1-Estimate updating ($N \geq N_{\text{init}}$)

$$\hat{\boldsymbol{b}}_{N+1}^{\text{ref}} = \hat{\boldsymbol{b}}_N^{\text{ref}} + \boldsymbol{K}_{N+1} \left(\begin{bmatrix} y_{1,N+1} \\ \vdots \\ y_{P,N+1} \end{bmatrix} - \boldsymbol{\rho} \boldsymbol{g}_{N+1} \hat{\boldsymbol{b}}_N^{\text{ref}} \right)$$

with

$$m_{N+1}^{-1} = \boldsymbol{\rho}^T \begin{bmatrix} r_{1,N+1}^{-1} & & 0 \\ & \ddots & \\ 0 & & r_{P,N+1}^{-1} \end{bmatrix} \boldsymbol{\rho}$$

$$\boldsymbol{C}_{N+1} = \boldsymbol{P}_N \boldsymbol{g}_{N+1}^T (m_{N+1} + \boldsymbol{g}_{N+1} \boldsymbol{P}_N \boldsymbol{g}_{N+1}^T)^{-1}$$

$$\boldsymbol{K}_{N+1} = m_{N+1} \boldsymbol{C}_{N+1} \begin{bmatrix} r_{1,N+1}^{-1} & & 0 \\ & \ddots & \\ 0 & & r_{P,N+1}^{-1} \end{bmatrix}$$

2-Covariance error calculation ($N \geq N_{init}$)

$$\boldsymbol{P}_{N+1} = \left(\boldsymbol{I} - \boldsymbol{C}_{N+1} \boldsymbol{g}_{N+1}\right) \boldsymbol{P}_{N+1}$$

References

[1] Lachapelle, G., Petovello, M., Gao, Y. and Garin, L., *Precise Point Positioning and its Challenges, Aided-GPS and Signal Tracking*, Inside GNSS, November/December 2006.

[2] Sklar, B.. *Digital Communications, Fundamentals and Applications*. Prentice Hall, New Jersey, 1988.

[3] Roncagliolo, P. A., Garcia, J. G., “High Dynamics and False Lock Resistant GNSS Carrier Tracking Loops,” Proc. of the 20th International Technical Meeting of the Satellite Division of The Institute of Navigation (ION GNSS 2007), Fort Worth, TX, September 2007.

[4] Eynard, G., Laot, C., ”Extended linear phase detector characteristic of a software PLL,” Communications, Control and Signal Proc., 2008. ISCCSP 2008. 3rd International Symposium on , vol., no., pp.62,67, 12-14 March 2008

[5] Roche, S., Bidon, S., Besson, O., Monnerat, M., Ries, L., Thevenon, P., “PLL Unwrapping Structures using Polynomial Prediction Algorithm for Noisy Carrier Phase Tracking,” Proc. of the 25th International Technical Meeting of The Satellite Division of the Institute of Navigation (ION GNSS 2012), Nashville, TN, September 2012.

[6] B. W. Parkinson , J. J. Spilker , P. Axelrad and P. Enge Global Positioning System: Theory and Applications, vol. I, pp.58 1996 :American Institute of Aeronautics and Astronautics

[7] Ziedan, N. I., “Multi-Frequency Combined Processing for Direct and Multipath Signals Tracking Based on Particle Filtering,” Proc. of the 24th International Technical Meeting of The Satellite Division of the Institute of Navigation (ION GNSS 2011), Portland, OR, September 2011.

[8] Henkel, P., Giger, K., Gunther, C., “Multifrequency, Multisatellite Vector Phase-Locked Loop for Robust Carrier Tracking,” Selected Topics in Signal Proc., IEEE Journal of , vol.3, no.4, pp.674,681, Aug. 2009

[9] Sahmoudi, M., Landry, R., Gagnon, F., “Robust mitigation of multipath and ionospheric delays in multi-GNSS real-time kinematic (RTK) receivers,” Statistical Signal Processing, 2009. SSP ’09. IEEE/SP 15th Workshop on , vol., no., pp.149,152, Aug. 31 2009-Sept. 3 2009

[10] ED Kaplan, Understanding GPS Principles and Applications, Artech House Publishers (1995)

[11] Christie, J. R. I., Parkinson, B. W., Enge, P. K., “The Effects of the Ionosphere and C/A Frequency on GPS Signal Shape: Considerations for GNSS-2,” Proc. of the 9th International Technical Meeting of the Satellite Division of The Institute of Navigation (ION GPS 1996), Kansas City, MO, September 1996.

[12] Steven M. Kay. Fundamentals of Statistical Signal Proc. : Estimation Theory. Prentice Hall, 1993.

[13] Falletti, E., Pini, M., Presti, L.L., “Low Complexity Carrier-to-Noise Ratio Estimators for GNSS Digital Receivers,” IEEE Transactions on Aerospace and Electronic Systems, vol.47, no.1, pp.420,437, January 2011

[14] Global Positionning System Wing (GPSW) Systems Engineering and Integration, Interface Specification, IS-GPS-200, Revision E, www.gps.gov